Acta Crystallographica Section B
Structural Science
ISSN 0108-7681

X-ray studies of crystalline complexes involving amino acids and peptides. XLIV. Invariant features of supramolecular association and chiral effects in the complexes of arginine and lysine with tartaric acid

M. Selvaraj, S. Thamotharan, Siddhartha Roy and M. Vijayan*

Molecular Biophysics Unit, Indian Institute of Science, Bangalore 560 012, India

Correspondence e-mail: mv@mbu.iisc.ernet.in

Received 10 October 2006
Accepted 9 March 2007

Part XLIII: Sharma *et al.* (2006).

The tartaric acid complexes with arginine and lysine exhibit two stoichiometries depending upon the ionization state of the anion. The structures reported here are DL-argininium DL-hydrogen tartrate, bis(L-argininium) L-tartrate, bis(DL-lysinium) DL-tartrate monohydrate, L-lysinium D-hydrogen tartrate and L-lysinium L-hydrogen tartrate. During crystallization, L-lysine preferentially interacts with D-tartaric acid to form a complex when DL-tartaric acid is used in the experiment. The anions and the cations aggregate into separate alternating layers in four of the five complexes. In bis(L-argininium) L-tartrate, the amino acid layers are interconnected by individual tartrate ions which do not interact among themselves. The aggregation of argininium ions in the DL- and the L-arginine complexes is remarkably similar, which is in turn similar to those observed in other dicarboxylic acid complexes of arginine. Thus, argininium ions have a tendency to assume similar patterns of aggregation, which are largely unaffected by a change in the chemistry of partner molecules such as the introduction of hydroxyl groups or a change in chirality or stoichiometry. On the contrary, the lysinium ions exhibit fundamentally different aggregation patterns in the DL–DL complexes on the one hand and L–D and L–L complexes on the other. Interestingly, the pattern in the L–D complex is similar to that in the L–L complex. The lysinium ions in the DL–DL complex exhibit an aggregation pattern similar to those observed in the DL-lysine complexes involving other dicarboxylic acids. Thus, the effect of change in the chirality of a subset of the component complexes could be profound or marginal, in an unpredictable manner. The relevant crystal structures appear to indicate that the preference of L-lysine for D-tartaric acid is perhaps caused by chiral discrimination resulting from the amplification of a small energy difference.

1. Introduction

A long-range program aimed at elucidating, at atomic resolution, the geometrical features of possible biologically relevant interactions, which is being pursued in this laboratory, involves the preparation and X-ray analysis of crystalline complexes of amino acids and peptides (Roy *et al.*, 2005; Sharma *et al.*, 2006, and references therein). Since the recognition of the possible implications to chemical evolution of the results obtained, particularly to prebiotic polymerization and

Table 1
Crystal data, details of data collection and refinement parameters.

	(I)	(II)	(III)	(IV)	(V)
Crystal data					
Chemical formula	$C_6H_{15}N_4O_2^+\cdot C_4H_5O_6^-$	$2C_6H_{15}N_4O_2^+\cdot C_4H_4O_6^{2-}$	$2C_6H_{15}N_4O_2^+\cdot\cdot C_4H_4O_6^{2-}\cdot H_2O$	$C_6H_{15}N_2O_2^+\cdot C_4H_5O_6^-$	$C_6H_{15}N_2O_2^+\cdot C_4H_5O_6^-$
M_r	324.30	498.51	460.49	296.28	296.28
Cell setting, space group	Triclinic, $P\overline{1}$	Monoclinic, $P12_11$	Monoclinic, $P2_1/c$	Monoclinic, $P12_11$	Monoclinic, $P12_11$
Temperature (K)	298 (2)	298 (2)	298 (2)	2983 (2)	298 (2)
a, b, c (Å)	5.4876 (16), 10.021 (3), 13.868 (4)	9.907 (2), 8.7428 (18), 14.076 (3)	10.087 (3), 23.003 (8), 9.414 (3)	5.1849 (11), 16.667 (4), 7.6701 (17)	5.1022 (11), 17.444 (4), 7.547 (2)
α, β, γ (°)	109.079 (5), 94.378 (5), 94.538 (5)	90.00, 109.412 (3), 90.00	90.00, 90.820 (7), 90.00	90.00, 96.366 (4), 90.00	90.00, 97.748 (4), 90.00
V (Å^3)	714.3 (4)	1149.9 (4)	2184.2 (13)	658.7 (2)	665.6 (3)
Z	2	2	4	2	2
D_x (Mg m^{-3})	1.508	1.440	1.400	1.494	1.478
Radiation type	Mo $K\alpha$	Mo $K\alpha$	Mo $K\alpha$	Mo $K\alpha$	Mo $K\alpha$
μ (mm^{-1})	0.13	0.12	0.12	0.13	0.13
Crystal form, colour	Plate, colourless	Plate, colourless	Needle, colourless	Plate, colourless	Plate, colourless
Crystal size (mm)	0.25 × 0.2 × 0.1	0.42 × 0.27 × 0.15	0.47 × 0.10 × 0.07	0.4 × 0.35 × 0.2	0.35 × 0.25 × 0.20
Data collection					
Diffractometer	Bruker SMART CCD area detector	Bruker SMART CCD area detector	Bruker SMART CCD area detector	Bruker SMART CCD area detector	Bruker SMART CCD area detector
Data collection method	φ and ω scan	φ and ω scan	φ and ω scan	φ and ω scan	φ and ω scan
Absorption correction	None	None	None	None	None
No. of measured, independent and observed reflections	6914, 2504, 1543	8353, 2162, 2054	15 605, 3842, 2876	4251, 1342, 1231	3396, 1200, 1146
Criterion for observed reflections	$I > 2\sigma(I)$	$I > 2\sigma(I)$	$I > 2\sigma(I)$	$I > 2\sigma(I)$	$I > 2\sigma(I)$
R_{int}	0.057	0.016	0.046	0.025	0.028
θ_{max} (°)	25.0	25.0	25.0	26.0	25.0
Refinement					
Refinement on	F^2	F^2	F^2	F^2	F^2
$R[F^2 > 2\sigma(F^2)]$, $wR(F^2)$, S	0.062, 0.132, 1.07	0.034, 0.088, 1.06	0.071, 0.218, 1.10	0.040, 0.090, 1.13	0.048, 0.116, 1.13
No. of reflections	2508	2162	3842	1342	1200
No. of parameters	260	380	379	242	288
H-atom treatment	Mixture of independent and constrained refinement	Mixture of independent and constrained refinement	Mixture of independent and constrained refinement	Mixture of independent and constrained refinement	Mixture of independent and constrained refinement
Weighting scheme	$w = 1/[\sigma^2(F_o^2) + (0.0496P)^2 + 0.0651P]$, where $P = (F_o^2 + 2F_c^2)/3$	$w = 1/[\sigma^2(F_o^2) + (0.0559P)^2 + 0.2589P]$, where $P = (F_o^2 + 2F_c^2)/3$	$w = 1/[\sigma^2(F_o^2) + (0.1191P)^2 + 1.8406P]$, where $P = (F_o^2 + 2F_c^2)/3$	$w = 1/[\sigma^2(F_o^2) + (0.0479P)^2 + 0.0738P]$, where $P = (F_o^2 + 2F_c^2)/3$	$w = 1/[\sigma^2(F_o^2) + (0.0484P)^2 + 0.3283P]$, where $P = (F_o^2 + 2F_c^2)/3$
$(\Delta/\sigma)_{max}$	<0.0001	<0.0001	<0.0001	<0.0001	0.001
$\Delta\rho_{max}$, $\Delta\rho_{min}$ (e Å^{-3})	0.27, −0.23	0.37, −0.17	0.75, −0.30	0.15, −0.16	0.25, −0.19
Extinction method	None	*SHELXL*	None	None	None
Extinction coefficient	–	0.0074 (19)	–	–	–

Computer programs used: *SMART*, *SAINT* (Bruker, 2001), *SHELXS*97, *SHELXL*97 (Sheldrick, 1997), *ORTEP*3 (Farrugia, 1997), *PyMOL* (DeLano, 2002), *PLATON* (Spek, 2003).

chiral discrimination (Vijayan, 1980, 1988), the emphasis in the program has been on complexes between amino acids with basic side-chains and carboxylic acids which are believed to have existed in the prebiotic milieu. It was realised that the approach involving crystalline complexes was ideally suited to exploring the different modes of association of amino acids and carboxylic acids. Studies on complexes have yielded a wealth of information about the characteristic interaction and aggregation patterns, which are to some extent predictable, and chiral discrimination through non-covalent interactions. The studies also brought to light the effect of chirality not only on molecular aggregation, but also on the ionization state and the stoichiometry of the complexes.

Thus far the carboxylic acids used for complexation with L- and DL- arginine, lysine and histidine are formic (Suresh & Vijayan, 1995*a*,*b*) and acetic (Suresh *et al.*, 1994) acids, and the dicarboxylic oxalic (Chandra *et al.*, 1998), malonic (Saraswathi & Vijayan, 2002), maleic (Pratap *et al.*, 2000), succinic (Prasad & Vijayan, 1993), glutaric (Saraswathi & Vijayan, 2001), adipic (Roy *et al.*, 2005; Sharma *et al.*, 2006) and pimelic (Saraswathi *et al.*, 2003) acids. The only hydroxy carboxylic acid used so far has been glycolic acid, which contains one carboxyl and one

hydroxyl function. Complexes of only L- and DL-histidine with glycolic acid could be crystallized. However, analysis of these complexes provided the only instance of chiral separation through interactions with an achiral entity (Suresh & Vijayan, 1996). Attempts at the preparation of crystalline complexes involving L-, D- and DL-arginine and lysine, on the one hand, and L-, D- and DL-tartaric acid on the other, and structures of the resulting crystals, are reported here. The tartaric acid molecule contains two carboxyl and two hydroxyl functions. It is a well known chiral compound and is well suited to explore chiral effects. The complexes involving tartaric acid are also useful for delineating the effect of hydroxyl groups on supramolecular association involving amino and dicarboxylic acids. The structures of the tartaric acid complexes of histidine have already been reported (Marchewka *et al.*, 2003; Johnson & Feeder, 2004*a*,*b*).

2. Materials and methods

The amino acids and the tartaric acids used in the investigation were obtained from Sigma Chemical Company. Crystals were grown by liquid diffusion of organic solvents into aqueous solutions of the components, mostly in a molar ratio. In the case of lysine, all combinations of L-, D- and DL-lysine on the one hand, and L-, D- and DL-tartaric acid on the other, were explored. It was verified that enantiomorphous complexes (for example that between L-lysine and D-tartaric acid, and that between D-lysine and L-tartaric acid) yielded crystals with identical space groups and cell parameters. In the case of arginine, crystallization experiments were carried out using L-arginine with L-, D- and DL-tartaric acid and DL-arginine with DL-tartaric acid. The precipitants used in the experiments which yielded complex crystals are methanol (L-lysine and D-tartaric acid, L-lysine and L-tartaric acid), propanol (DL-lysine

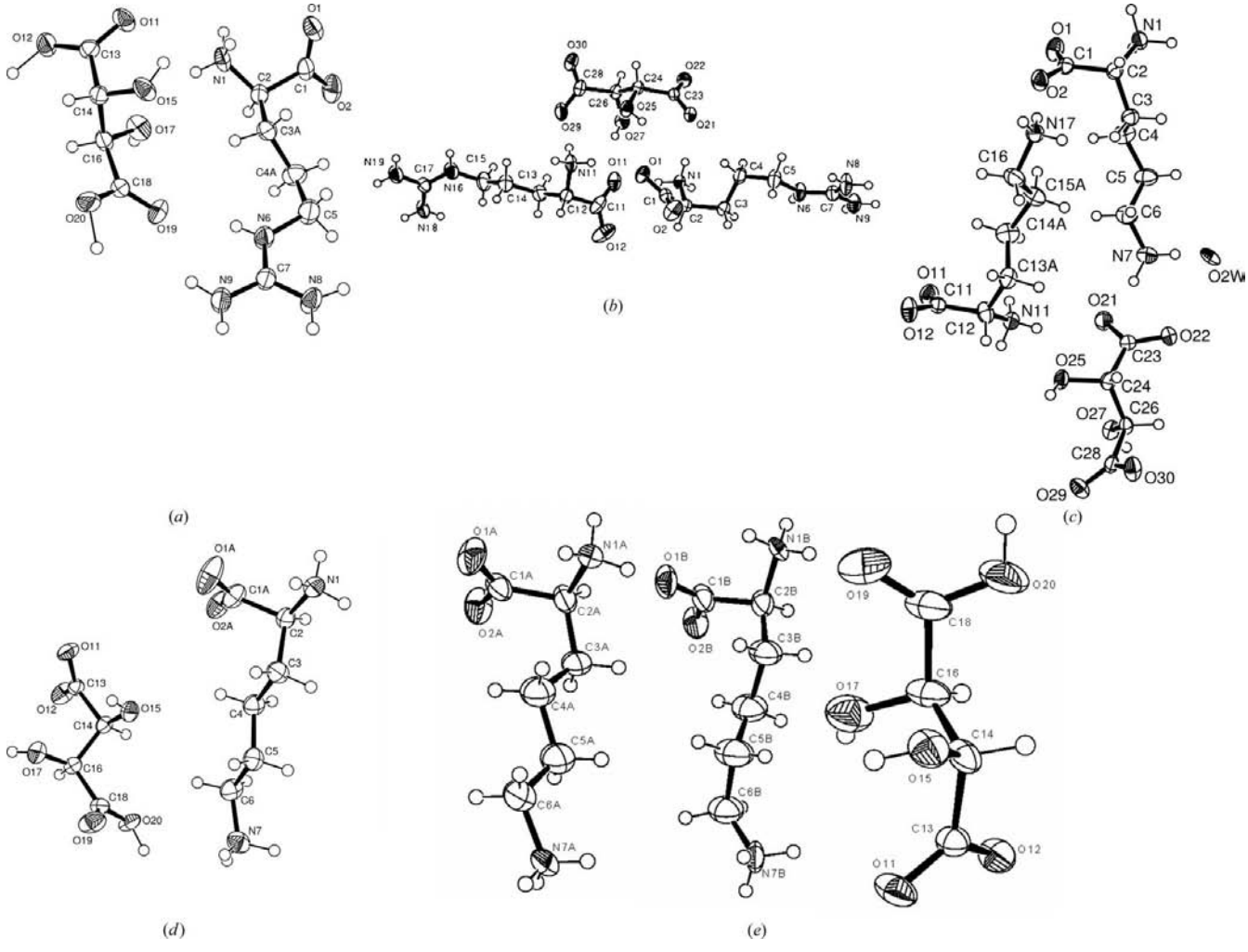

Figure 1
Ellipsoid plots of the components of the crystal structures. In the event of disorder, only the major component is illustrated, except in the case of (V) [part (*e*)]. *A* and *B* denote major and minor components, respectively. The displacement ellipsoids are at the 50% probability level. (*a*) DL-argininium DL-hydrogen tartrate (I), (*b*) bis(L-argininium) L-tartrate (II), (*c*) bis(DL-lysinium) DL-tartrate monohydrate (III), (*d*) L-lysinium D-hydrogen tartrate (IV) and (*e*) L-lysinium L-hydrogen tartrate (V).

Table 2
Hydrogen-bond parameters (Å, °) in DL-argininium DL-hydrogen tartrate.

D—H···A	d(H···A)	d(D···A)	D—H···A
N1—H1A···O1^{i}	1.74 (5)	2.788 (4)	169 (3)
N1—H1B···O17	2.21 (4)	3.001 (4)	160 (3)
N1—H1C···O1^{ii}	2.29 (6)	3.171 (4)	141 (4)
N1—H1C···O2^{ii}	2.31 (6)	3.300 (4)	159 (4)
N6—H6···O19	2.11 (4)	2.892 (4)	155 (4)
N8—H8A···O2^{iii}	1.91 (4)	2.807 (4)	155 (3)
N8—H8B···O11^{iv}	1.89 (4)	2.801 (4)	174 (4)
N9—H9A···O12^{iv}	2.25 (4)	3.099 (4)	176 (3)
N9—H9B···O19	2.34 (4)	3.111 (5)	145 (3)
N9—H9B···O20^{v}	2.33 (4)	2.976 (4)	129 (3)
O12—H12···O12^{vi}	1.225	2.451 (4)	180
O15—H15···O1^{i}	2.02 (5)	2.813 (3)	144 (4)
O17—H17···O20^{vii}	2.13	2.953 (4)	178
O20—H20···O20^{v}	1.233	2.466 (4)	180

Symmetry codes: (i) $-x, -y+1, -z+2$; (ii) $-x-1, -y+1, -z+2$; (iii) $-x, -y+2, -z+2$; (iv) $x+1, y+1, z$; (v) $-x+1, -y+1, -z+1$; (vi) $-x, -y, -z+1$; (vii) $x-1, y, z$.

and DL-tartaric acid), butanol (L-arginine and L-tartaric acid) and acetonitrile (DL-arginine and DL-tartaric acid).

Of the crystals grown, the structure of the complex between L-lysine and L-tartaric acid has already been reported (Debrus *et al.*, 2005). (The refcodes of the two polymorphs are CAVCUY and CAVCUY01, but no coordinates were in the CSD , Allen, 2002, at the time of the submission of this paper.) However, the structure was redetermined and refined using crystals grown in the present study. This was done to ensure that crystals grown under identical conditions were used when comparing L–L and L–D complexes.

Crystal data, details of data collection and refinement statistics are given in Table 1. The resolution of data sets is not very high, but they are comparable to those obtained from crystals of similar complexes. In any case, it is adequate to reliably describe supramolecular association in the crystals. All the five structures were solved by direct methods using *SHELXS*97 (Sheldrick, 1997) and refined by the full-matrix least-squares method using *SHELXL*97 (Sheldrick, 1997). Atoms C3 and C4 are disordered over two alternate positions with site-occupation factors of 0.825 (5) for the major component in DL-argininium DL-hydrogen tartrate. In bis(DL-lysinium) DL-tartrate monohydrate, three atoms of one of the lysinium ions (C13, C14 and C15) were disordered over two sites each, with site-occupation factors of 0.765 (7) for the major conformation, while the lone water molecule is disordered over three locations with occupancy factors of 0.33, 0.34 and 0.33, respectively. A minor component with an occupancy of 0.185 (11) exists for the carboxylate group (C1, O1 and O2) in L-lysinium D-hydrogen tartrate. The entire lysinium ion in the corresponding L–L complex is disordered with an occupancy of 0.608 (6) for the major component and 0.392 (6) for the minor component. Similarity restraints were applied to all 1,2- and 1,3-distances involving disordered atoms, so as to maintain similar geometry about the chemically equivalent atoms. The non-H atoms including disordered water molecules were refined anisotropically. In DL-argininium DL-hydrogen tartrate, each carboxyl group of the anion is involved in a symmetric hydrogen bond with its centrosymmetric equivalent, with the H atom located at its inversion centre. Therefore, the structure contains two H atoms located at inversion centres. Only their isotropic displacement parameters were refined. All the H atoms attached to N and O, except those attached to the disordered amino groups, were located in difference maps. Among them, all except those attached to O27 in DL-lysinium DL-tartrate and O17 in L-lysinium D-hydrogen tartrate were refined freely. H atoms attached to C atoms were fixed with the aid of geometrical considerations. These and the H atoms attached to O27 and O17 were treated as riding on their parent atoms. In the case of bis(L-argininium) L-tartrate and DL-argininium DL-tartrate, bond-length restraints were applied to O25—H25 and O17—H17 bonds. Lengths and angle constraints were used to refine H atoms geometrically fixed to disordered N atoms. Friedel pairs were merged during final refinement. The absolute configurations of the molecules were deduced from those of the components.

3. Results and discussion

3.1. Chiral discrimination, ionization state and stoichiometry

Crystallization experiments involving L-lysine and DL-tartaric acid yielded a complex between the L amino acid and D-tartaric acid. Crystals of the complex could not be obtained from similar experiments involving arginine. Thus, L-lysine appears to interact preferentially with D-tartaric acid. However, the interactions of the amino acid with tartaric acid is strong enough to form L–L complexes where the choice of D-tartaric acid is not offered.

In all the crystals, the amino acid exists as a singly, positively charged zwitterion with a positively charged α-amino group, a negatively charged α-carboxylate group and a positively charged side-chain amino or guanidyl group. Hydrogen tartrate is formed in all complexes except two, in each of which a tartrate ion exists. In the latter event, understandably, the stoichiometry between the amino acid and the tartrate ion is 2:1. In DL-argininium DL-hydrogen tartrate, both the carboxyl groups of the hydrogen tartrate ion formally carry half a hydrogen each. Each of them is involved in a symmetric O···O hydrogen bond with its centrosymmetric equivalent. Tartaric acid is obtained when the two central C atoms in succinic acid are hydroxylated. However, the variation in ionization state and stoichiometry exhibited by amino acid–tartaric acid complexes is lower than that exhibited by the corresponding succinic acid complexes (Prasad & Vijayan, 1993). Furthermore, a weak correlation between chirality and stoichiometry could be established in the succinic acid complexes. No such correlation appears to exist in the tartaric acid complexes.

In light of the above discussion, the structures reported here can be described as DL-argininium DL-hydrogen tartrate (I), bis(L-argininium) L-tartrate (II), bis(DL-lysinium) DL-tartrate monohydrate (III), L-lysinium D-hydrogen tartrate (IV) and L-

Table 3
Hydrogen-bond parameters (Å, °) in bis(L-argininium) L-tartrate.

D—H···A	d(H···A)	d(D···A)	D—H···A
N1—H1A···O21	2.01 (4)	2.892 (3)	171 (3)
N1—H1B···O11	1.82 (4)	2.759 (3)	177 (3)
N1—H1C···O22^{i}	1.86 (3)	2.770 (3)	176 (3)
N6—H6···O27^{i}	1.91 (3)	2.785 (3)	164 (3)
N8—H8A···O12^{ii}	2.16 (4)	2.961 (4)	167 (4)
N8—H8B···O21^{iii}	2.15 (3)	2.934 (3)	155 (3)
N9—H9A···O29^{i}	2.30 (4)	3.130 (4)	162 (3)
N9—H9B···O21^{iii}	2.33 (4)	3.127 (4)	151 (3)
N11—H11A···O1	2.22 (4)	3.046 (3)	166 (4)
N11—H11B···O30^{iv}	1.81 (3)	2.732 (3)	170 (3)
N11—H11C···O29	1.99 (5)	2.906 (4)	176 (3)
N16—H16···O2^{v}	1.92 (3)	2.781 (3)	162 (3)
N18—H18A···O1^{vi}	2.00 (4)	2.863 (3)	165 (3)
N18—H18B···O29^{vii}	1.86 (4)	2.840 (3)	168 (3)
N19—H19A···O2^{v}	2.03 (4)	2.841 (4)	149 (3)
N19—H19B···O29^{vii}	2.52 (5)	3.224 (4)	136 (4)
O25—H25···O1	2.23	2.840 (3)	131
O27—H27···O11	1.89 (5)	2.698 (4)	155 (4)

Symmetry codes: (i) $-x+1, y+\frac{1}{2}, -z+1$; (ii) $x-1, y, z$; (iii) $-x, y+\frac{1}{2}, -z+1$; (iv) $-x+2, y+\frac{1}{2}, -z+2$; (v) $-x+2, y-\frac{1}{2}, -z+2$; (vi) $x+1, y, z$; (vii) $-x+3, y+\frac{1}{2}, -z+2$.

Table 4
Hydrogen-bond parameters (Å, °) in bis(DL-lysinium) DL-tartrate monohydrate.

D—H···A	d(H···A)	d(D···A)	D—H···A
N1—H1A···O30^{i}	1.90 (5)	2.879 (4)	168 (4)
N1—H1B···O11^{ii}	2.00 (5)	2.938 (5)	151 (4)
N1—H1C···O2^{iii}	1.75 (5)	2.794 (4)	165 (4)
N7—H7A···O12^{iv}	1.90 (6)	2.852 (5)	169 (5)
N7—H7B···O21	1.77 (6)	2.774 (4)	169 (5)
N7—H7C···O1W	2.06 (4)	2.950 (9)	172 (4)
N7—H7C···O2W	2.30 (4)	2.956 (9)	130 (3)
N11—H11A···O1^{v}	2.36 (5)	3.146 (5)	149 (3)
N11—H11A···O2^{vi}	2.44 (4)	3.061 (4)	129 (3)
N11—H11B···O21	2.09 (6)	2.868 (4)	155 (5)
N11—H11B···O25	2.31 (5)	2.929 (4)	131 (4)
N11—H11C···O12^{iii}	1.98 (5)	2.872 (5)	174 (4)
N17—H17A···O27^{vii}	2.24 (5)	2.926 (4)	138 (4)
N17—H17A···O29^{vii}	2.25 (6)	2.983 (5)	144 (4)
N17—H17B···O30^{viii}	1.94 (6)	2.915 (5)	169 (4)
N17—H17C···O2	2.20 (5)	2.972 (5)	176 (4)
O25—H25···O29^{ix}	1.85 (6)	2.708 (4)	164 (5)
O27—H27···O22^{x}	1.90	2.702 (4)	167
O3W···O29^{x}	–	2.904 (1)	–
O3W···O1W^{xi}	–	3.030 (2)	–

Symmetry codes: (i) $-x+1, -y, -z+1$; (ii) $x-1, -y+\frac{1}{2}, z+\frac{1}{2}$; (iii) $x, -y+\frac{1}{2}, z+\frac{1}{2}$; (iv) $x, y, z+1$; (v) $x+1, -y+\frac{1}{2}, z-\frac{1}{2}$; (vi) $x+1, y, z$; (vii) $x-1, y, z$; (viii) $-x+1, -y, -z$; (ix) $-x+2, -y, -z$; (x) $-x+2, -y, -z+1$; (xi) $-x+1, -y, -z+2$.

lysinium L-hydrogen tartrate (V). The amino-acid conformations found in them (Fig. 1) have been observed previously (Saraswathi *et al.*, 2003; Roy *et al.*, 2005; Sharma *et al.*, 2006) and do not exhibit any special feature. In all the structures the torsion angle about the central C—C bond in tartrate/hydrogen tartrate is close to 180° corresponding to an extended conformation.

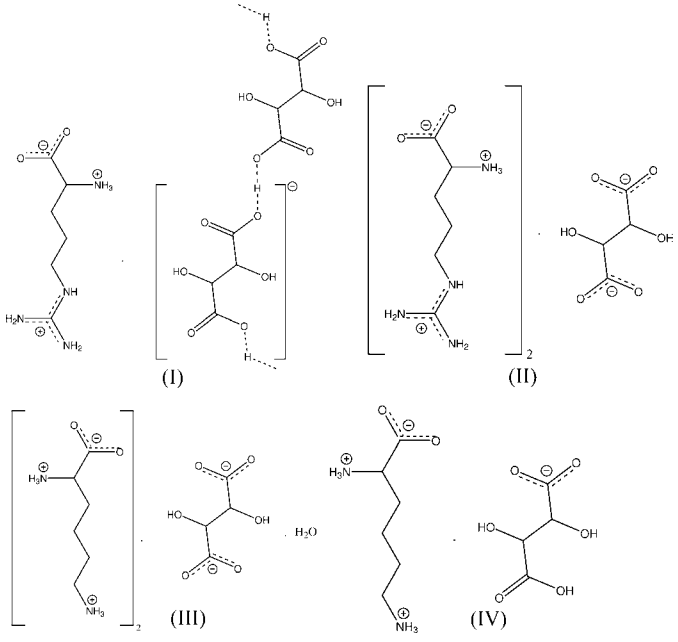

3.2. Crystal structure and molecular aggregation

All the structures are stabilized by networks of hydrogen bonds. The parameters of these hydrogen bonds are given in Tables 2–6. The argininium ion has four donors capable of forming eight hydrogen bonds, while lysinium can form six hydrogen bonds using two donors. All the donors are amino or guanidyl N atoms. In the five structures reported here, there are 48 potential hydrogen bonds with these donors. The potential is fully realised in 47 of them. The remaining one in L-lysinium L-hydrogen tartrate, involves the α-amino group of a disordered lysinium ion. In one of the two disordered components, the amino nitrogen is involved, as expected, in three hydrogen bonds. Two are clearly discernible in the other component, but the identification of a third would require considerable relaxation of the angle criterion, which is not unreasonable in view of the disorder. The two carboxylate O atoms in each amino acid zwitterion can be acceptors in hydrogen bonds. Among the 14 such O atoms in the structures reported here, 13 are acceptors in one or more hydrogen bond each. O1 in L-lysinium D-hydrogen tartrate is not involved in any hydrogen bond. Careful examination indicates this observation to be genuine. The carboxylate group bearing this oxygen can be, and has been, treated as disordered with a minor component having an occupancy of 0.185. The situation remains the same even if disorder is not invoked. The tartrate/hydrogen tartrate ions present a more complex situation with two possible ionization states, symmetric hydrogen bonds and the capability of hydroxyl O atoms to act as donors as well as acceptors. All the O atoms in the ions are involved in hydrogen bonds, but the potential of hydroxyl O atoms to act as acceptors is not always fulfilled. Each amino acid–tartaric acid complex contains a large number of hydrogen bonds and the observed structure results from the simultaneous optimization of all of them. Therefore, the absence of an expected hydrogen bond or departures from expected geometry cannot be ruled out, and indeed has been observed in similar

Table 5
Hydrogen-bond parameters (Å, °) in L-lysinium D-hydrogen tartrate.

O2*B* of the minor components are involved in the same hydrogen bonds as O2*A*.

D—H···*A*	*d*(H···*A*)	*d*(*D*···*A*)	*D*—H···*A*
N1—H1*A*···O12^{i}	2.22 (4)	2.959 (4)	141 (3)
N1—H1*A*···O17^{ii}	2.38 (4)	3.001 (4)	127 (3)
N1—H1*B*···O19^{iii}	1.99 (4)	2.890 (4)	169 (4)
N1—H1*C*···O2*A*^{iv}	2.00 (5)	2.849 (6)	169 (4)
N7—H7*A*···O2*A*^{v}	1.67 (5)	2.675 (5)	174 (4)
N7—H7*B*···O11^{v}	2.08 (5)	2.870 (4)	156 (4)
N7—H7*C*···O12^{vi}	2.38 (5)	3.095 (4)	135 (4)
O15—H15···O12^{iv}	1.95 (5)	2.808 (4)	170 (5)
O17—H17···O2*A*^{vii}	2.47	3.230 (7)	155
O20—H20···O11^{v}	1.57 (5)	2.528 (3)	171 (5)

Symmetry codes: (i) $-x+1, y+\frac{1}{2}, -z$; (ii) $-x, y+\frac{1}{2}, -z$; (iii) $-x, y+\frac{1}{2}, -z+1$; (iv) $x-1, y, z$; (v) $x, y, z+1$; (vi) $x-1, y, z+1$; (vii) $-x+1, y-\frac{1}{2}, -z$.

Table 6
Hydrogen-bond parameters (Å, °) in L-lysinium L-hydrogen tartrate.

D—H···*A*	*d*(H···*A*)	*d*(*D*···*A*)	*D*—H···*A*
Major component			
N1*A*—H*A*1*B*···O17^{i}	2.32	3.119 (13)	149
N1*A*—H*A*1*C*···O19^{ii}	1.97	2.862 (13)	177
N7*A*—H*A*7*A*···O12^{iii}	2.41	3.160 (2)	141
N7*A*—H*A*7*B*···O2*A*^{iv}	1.92	2.720 (3)	149
N7*A*—H*A*7*C*···O1*A*^{v}	2.32	3.100 (2)	145
N7*A*—H*A*7*C*···O2*A*^{v}	2.02	2.790 (2)	145
O15—H15···O12^{vi}	1.93 (5)	2.736 (4)	160 (4)
O17—H17···O1*A*^{v}	1.86 (8)	2.742 (12)	172 (7)
O20—H20···O11^{vii}	1.63 (9)	2.533 (4)	175 (9)
Minor component			
N1*B*—H*B*1*A*···O12^{vii}	2.00	2.753 (19)	142
N1*B*—H*B*1*B*···O17^{i}	2.04	2.884 (19)	157
N1*B*—H*B*1*C*···O19^{ii}	1.95	2.800 (2)	160
N7*B*—H*B*7*A*···O2*B*^{v}	2.16	3.020 (3)	162
N7*B*—H*B*7*B*···O11^{viii}	1.92	2.710 (2)	146
N7*B*—H*B*7*C*···O2*B*^{iv}	2.36	3.170 (4)	151
O15—H15···O12^{vi}	1.93 (5)	2.736 (4)	160 (4)
O17—H17···O1*B*^{v}	1.82 (8)	2.678 (18)	164 (7)
O20—H20···O11^{vii}	1.63 (9)	2.533 (4)	175 (9)

Symmetry codes: (i) $x-1, y, z-1$; (ii) $x-1, y, z$; (iii) $-x, y+\frac{1}{2}, -z+2$; (iv) $x+1, y, z+1$; (v) $x, y, z+1$; (vi) $x+1, y, z$; (vii) $x, y, z-1$; (viii) $-x+1, y+\frac{1}{2}, -z+2$. The possibility of a N1*A*—H*A*1*A*···O12^{vii} hydrogen bond exists with *d*(H···*A*) = 2.45 Å, *d*(*D*···*A*) = 2.870 (11) Å and ∠*D*—H···*A* = 110°, if the angle criterion is substantially relaxed.

complexes, although such absence and departures should be carefully examined to ensure that they are genuine within the confidence level of structure determination.

The crystal structure of DL-argininium DL-hydrogen tartrate is given in Fig. 2(*a*). As in the case of many other amino acid complexes analysed in this laboratory, the cations and the anions aggregate into separate alternating layers and the layers are stacked along the longest cell dimension. The amino acid layer is parallel to the *ab* plane and is at around $z = 0$ (Fig. 2*b*), while the hydrogen tartrate layer parallel to the same plane is at around $z = 1/2$ (Fig. 2*c*). The argininium ions first aggregate into linear arrays of alternating L and D molecules. Each argininium ion interacts with another on one side through two N1···O1 hydrogen bonds related by an inversion centre. On the other side, the interaction involves an N8···O2

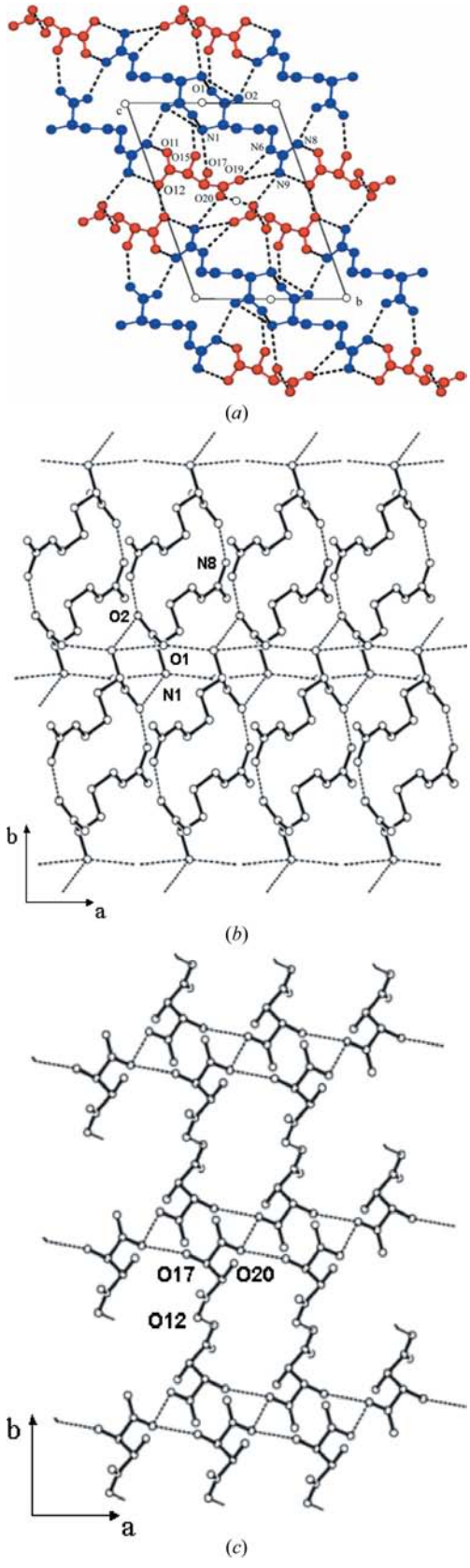

Figure 2
(*a*) Crystal structure of DL-argininium DL-hydrogen tartrate. Unless otherwise stated, the anions and cations are represented in red and blue, respectively, in this and the other crystal structure diagrams. (*b*) The argininium layer; (*c*) the hydrogen tartrate layer.

hydrogen bond and its centrosymmetric equivalent. Thus, the array involves two types of 'dimerization', one stabilized by hydrogen bonds between α-amino and α-carboxyl groups and the other by those between α-carboxylate and side-chain guanidyl groups. In terms of Etter net (Etter *et al.*, 1990), the two hydrogen-bonded rings can be described as $R_2^2(10)$ and $R_2^2(20)$ graph-set motifs (Bernstein *et al.*, 1995). Adjacent arrays in the layer are interconnected only by a weak bifurcated hydrogen bond with N1 as the donor and O1 and O2 as acceptors (Table 2).

The hydrogen tartrate layer (Fig. 2*c*) also has a highly symmetric arrangement of molecules. O20 at one end of the molecular ion shares a hydrogen in a symmetric hydrogen bond with its centrosymmetric equivalent. At the other end, O12 has a similar interaction with its centrosymmetric equivalent. These two hydrogen bonds lead to a linear array of strongly interconnected hydrogen tartrate ions along the [110] direction, which may be assigned to the graph set *D*. The linear arrays are interconnected by a hydrogen bond between a hydroxyl oxygen (O17) in one array and a carboxylate oxygen (O20) in the other [graph-set motif of $C(5)$].

The interactions of the amino-acid layer with the hydrogen tartrate layer contain two specific interactions involving the guanidyl group. In one, N8 and N9 have a specific interaction (Salunke & Vijayan, 1981; Vijayan, 1988) made up of two parallel hydrogen bonds with two carboxylate O atoms at one end of the hydrogen tartrate ion. At the other end of the ion, O19 is the common acceptor of protons from N6 and N9. In addition, the α-amino N1 atom forms a hydrogen bond with the hydroxyl O17 atom and the hydroxyl O15 atom forms one with the α-carboxylate oxygen O1. Thus, the crystal structure of DL-argininium DL-hydrogen tartrate involves a highly symmetric and tightly interconnected arrangement of molecular ions.

The stoichiometry in the L–L complex between arginine and tartaric acid (Fig. 3*a*) is 2:1 rather than 1:1 which is found in the DL–DL complex, with a doubly charged tartrate ion compensating the positive charges on the two argininium ions. However, the basic element of aggregation, namely a linear array involving two modes of dimerization (Fig. 3*b*), involving the graph-set motifs $R_2^2(10)$ and $R_2^2(20)$, remains nearly the same in the two complexes, except that inversion centres are replaced by pseudo-twofold axes in the L–L complex. An array which is parallel to a^* pairs with a 2_1 screw-related array running in the opposite direction. The two are interconnected by the specific interactions of a guanidyl group (N16, N19) in one array with a carboxyl oxygen (O2) in the other. These interactions and their symmetry equivalents led to the formation of a corrugated layer parallel to the a^*b plane. These layers are stacked along *c*. As shown in Fig. 3(*c*), adjacent corrugated layers of argininium ions are interconnected by tartrate ions, which do not interact among themselves.

Unlike in the case of the DL-arginine complex with DL-tartaric acid, but as in that of L-arginine with L-tartaric acid, the DL-lysine complex with DL-tartaric acid has a stoichiometry of 2:1 and involves a doubly negatively charged tartrate ion. In the crystal structure (Fig. 4*a*) the molecular ions with opposite charges again stack into alternating layers parallel to the *ac* plane. As schematically illustrated in Fig. 4(*b*), the lysinium ions aggregate into double arrays stabilized by interactions involving α-amino and α-carboxylate groups. The basic unit in each array is a hydrogen-bonded dimer involving lysinium ions of the same chirality [$R_2^2(10)$ motif]. Adjacent dimers are related by a glide plane. Adjacent double arrays in the layer are interconnected by hydrogen bonds between the side-chain amino group in one array and a carboxylate oxygen in the other, and their symmetry equivalents.

The basic element of aggregation in the tartrate layer (Fig. 4*c*) is a linear array stabilized by O—H···O hydrogen bonds. The interactions involve alternating pairs of hydrogen bonds of two types, each giving rise to the graph-set motif $R_2^2(12)$.

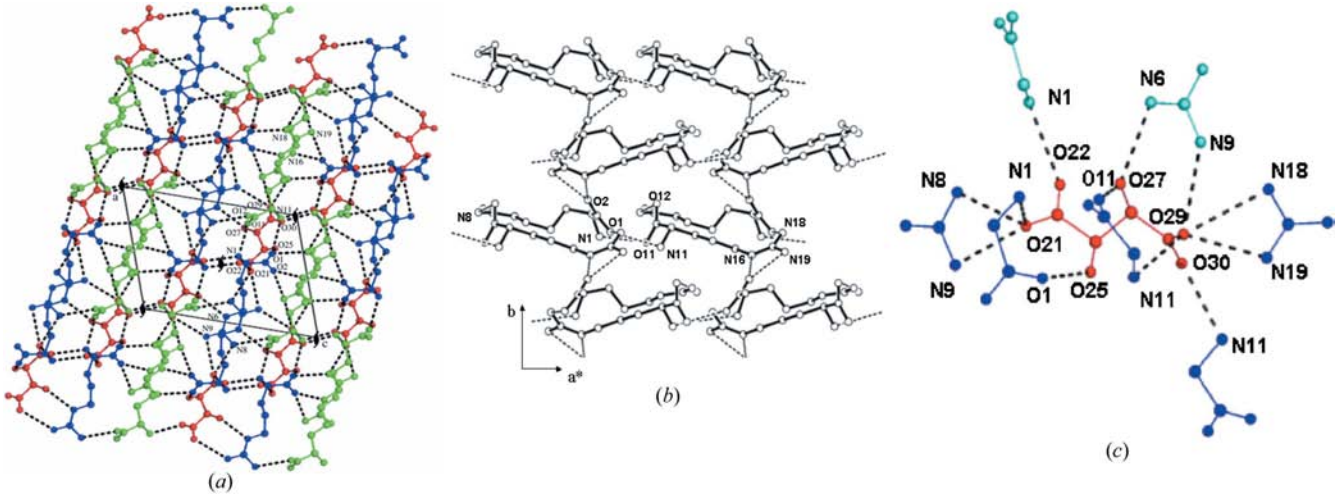

Figure 3
(*a*) Crystal structure of bis(L-argininium) L-tartrate. The two crystallographically independent argininium ions are given in blue and green. (*b*) The argininium layer; (*c*) tartrate–argininium interactions. Atoms in the argininium ions from adjacent layers are shown in different colours.

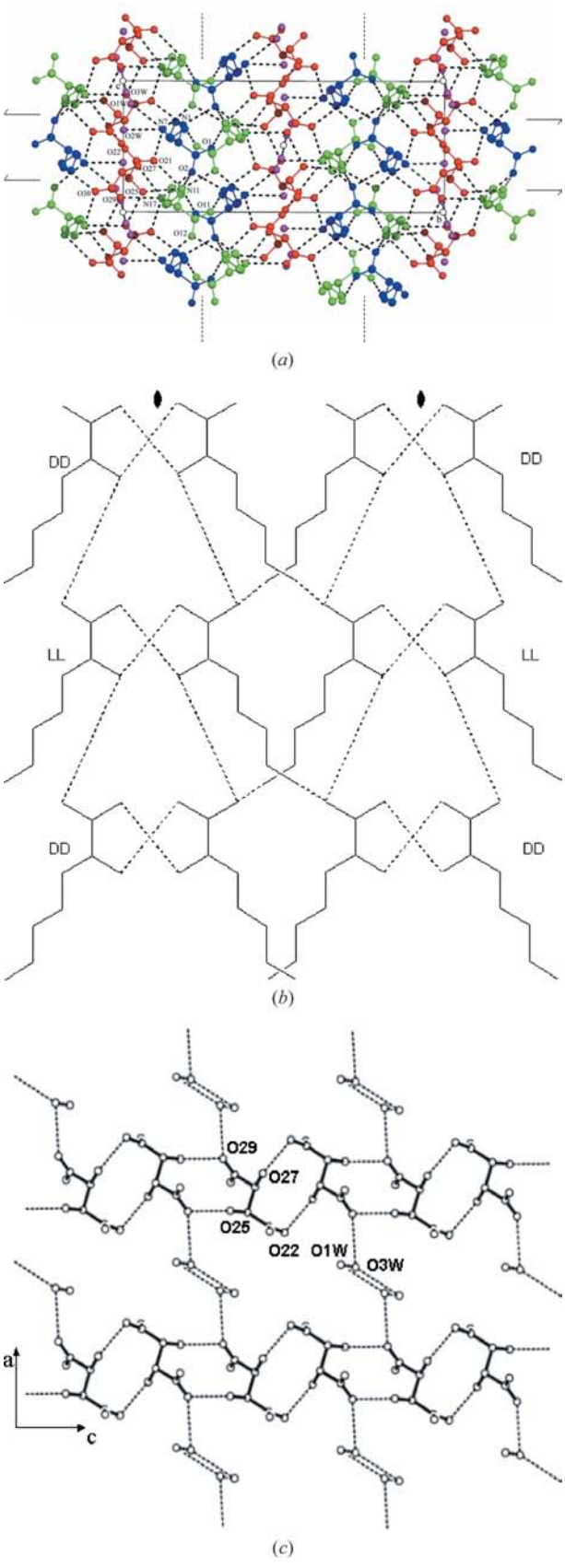

Figure 4
(*a*) Crystal structure of bis(DL-lysinium) DL-tartrate monohydrate. (*b*) Schematic illustration of the arrangement of lysinium ions in the layer. (*c*) The tartrate layer.

These are across inversion centres and both types of interactions are between hydroxyl and carboxylate groups of adjacent tartrate ions. The linear arrays are interconnected by a disordered water molecule and its symmetry equivalents. Hydrogen bonds involving both α-amino and side-chain amino groups of both the lysinium ions with tartrate O atoms are used in interactions between the amino acid and the tartrate layers. The side-chain amino group in one of the lysinium ions is also involved in a hydrogen bond with the disordered water molecule.

The positively charged and the negatively charged ions also aggregate into separate alternating layers in L-lysinium D-hydrogen tartrate (Fig. 5*a*). The lysinium layer exhibits a simple packing arrangement stabilized by two nearly perpendicular arrays of hydrogen bonds (Fig. 5*b*). The first, parallel to *a*, is made up of a hydrogen bond between the α-amino group of one lysinium ion, and an α-carboxylate oxygen (O2) of a translationally related ion and its symmetry equivalents [graph-set motif $C(5)$]. Using a nomenclature previously used often, this array constitutes an $S2$ head-to-tail sequence (Suresh & Vijayan, 1983). The second array parallel to *c* involves a hydrogen bond between the side-chain amino group of one ion and a carboxylate oxygen (the same as that which interacts with the α-amino group) of a translationally related ion, and its symmetry equivalents [graph-set motif $C(5)$]. The tartrate layer (Fig. 5*c*) is made up of linear arrays of hydrogen tartrates interconnected by O—H···O hydrogen bonds involving the carboxyl group of one ion and the carboxylate group of the neighboring ion [graph-set motif $C(7)$]. Adjacent arrays are interconnected by O—H···O hydrogen bonds involving a carboxylate group in one array and a hydroxyl group in another array [graph-set motif $C(5)$]. Interactions between adjacent layers involve both the amino group of the lysinium ion and the carboxyl, and the carboxylate groups and one of the hydroxyl groups of the hydrogen tartrate ion.

The crystal structure of L-lysinium L-hydrogen tartrate is remarkably similar to that of the L–D complex. The aggregation pattern in the hydrogen tartrate layer is exactly the same in both the structures, except for the change in the chirality of the ion. The pattern in the lysinium layer in the L–L complex (Fig. 5*d*) is very similar to that in the L–D complex, but exhibits subtle differences in hydrogen bonding. Essentially, a N1···O2 hydrogen bond in the latter is replaced by a N7···O2 hydrogen bond in the former. Differences in the lysinium–hydrogen tartrate interactions are also subtle. A hydrogen bond between a hydroxyl group of the hydrogen tartrate ion and a carboxylate oxygen of the lysinium ion exists in both complexes. In the L–D complex, there are four N—H···O hydrogen bonds between the ions. Two of them involve the α-amino group, one of which bifurcated, while the remaining two involve the side-chain amino group. The minor component of the lysinium ion in the L–L complex also makes four N—H···O hydrogen bonds with the hydrogen tartrate layer, three involving the α-amino group and one involving the side-chain amino group. There is some uncertainty about one of these hydrogen bonds in the major component.

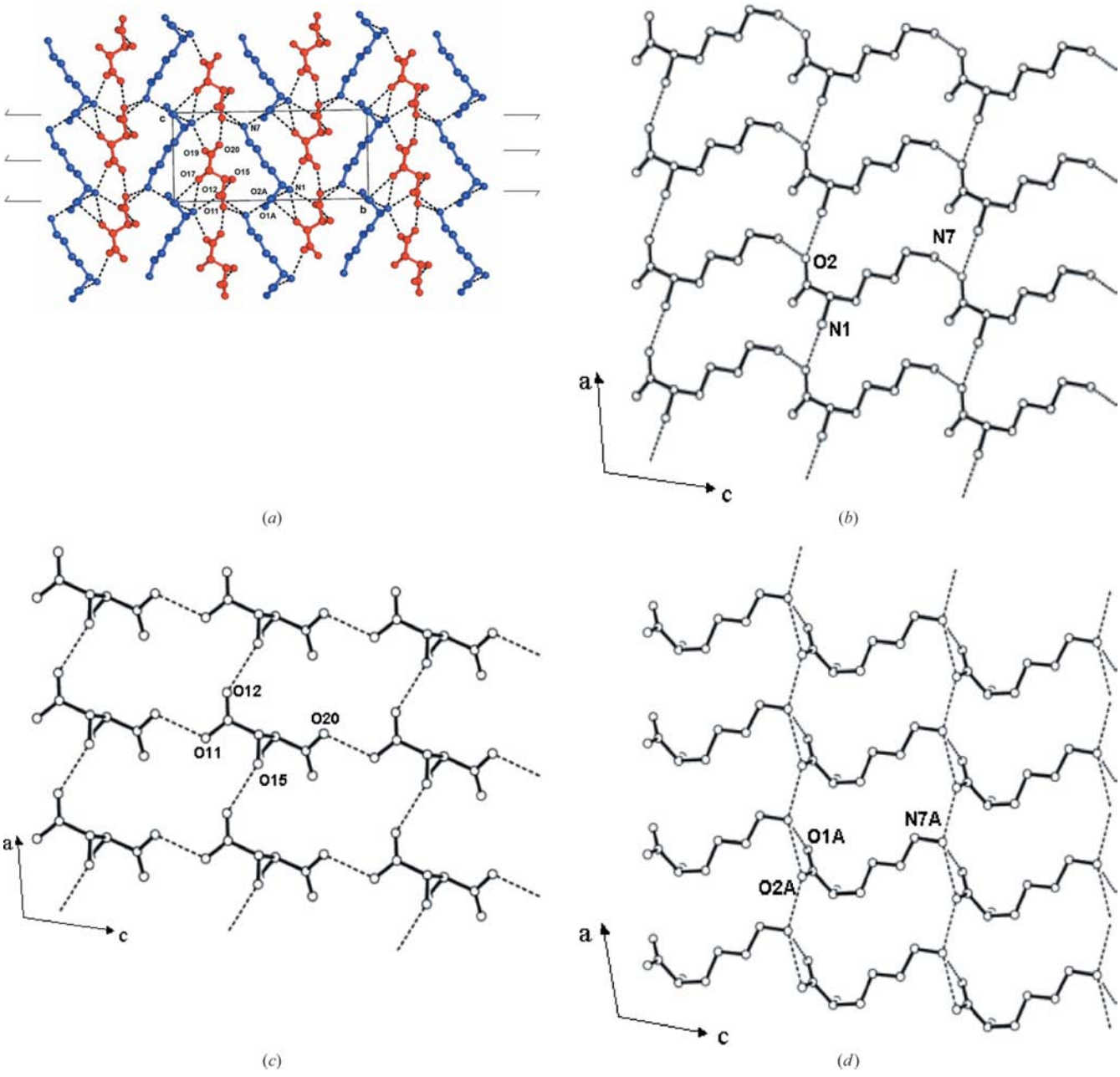

Figure 5
(*a*) Crystal structure of L-lysinium D-hydrogen tartrate. (*b*) The lysinium layer and (*c*) the hydrogen tartrate layer in the structure and (*d*) the amino acid layer (major component) in the L-lysinium L-hydrogen tartrate. The arrangement of the minor component is the same except that the bifurcated N7···O1/O2 hydrogen bond is replaced by a normal N7···O2 hydrogen bond.

3.3. Invariant features of supramolecular aggregation

The basic element of aggregation, namely an array involving two types of alternating dimeric interactions [graph-set motifs $R_2^2(10)$ and $R_2^2(20)$], is remarkably similar in the DL–DL and L–L complexes between arginine and tartaric acid, despite the differences in the chirality of the component molecules, the ionization state of one of them and the stoichiometry. The arrangement is also similar to that found in most complexes of arginine with larger dicarboxylic acids (Roy *et al.*, 2005). Thus, the results presented here show that the tendency of arginine to assume similar patterns of aggregation is largely unaffected by a change in the chemistry of the partner molecules such as the introduction of hydroxyl groups or a change in chirality or stoichiometry.

Unlike in the case of the two arginine complexes, the aggregation patterns of the amino acid in DL-lysinium DL-tartrate monohydrate and those in the L-lysinium complexes are fundamentally different. As in the case of DL-lysinium DL-tartrate monohydrate reported here, most of the DL-lysine complexes of carboxylic acids are characterized by the formation of double arrays and the interconnection of the double arrays through interactions involving hydrogen bonds between side-chain amino groups in one double array and the carboxylate groups in the other. However, there are differ-

ences in detail, particularly in relation to the use of symmetry elements. The aggregation pattern shows a higher variability in the L-lysine complexes of carboxylic acids.

The aggregation of tartrate/hydrogen tartrate ions in the structures reported here exhibits a variety of patterns. On the whole, the hydrogen tartrate ion exhibits a larger variability in aggregation than hydrogen succinate, and indeed other hydrogen dicarboxylates, in their amino acid complexes. This is presumably on account of the hydrogen-bonding possibilities introduced by the additional hydroxyl groups in hydrogen tartrate.

3.4. Chiral effects

The structures presented here confirm that the effect of a change in the chirality of the subset of the component molecules on molecular association could be profound in some instances or marginal in some others, in an unpredictable manner. It has not been possible to rationalize the observed effect in the amino acid complexes reported here and earlier. The carboxylic acids used so far in arginine, lysine and histidine complexes have been achiral. The tartaric acid molecule is, however, chiral. Interestingly, as explained in §2, given a choice, L-lysine preferentially interacts with D-tartaric acid. The L–D and the L–L complexes have the same space group with similar cell dimensions. The hydrogen tartrate layers in the two crystals have almost the same structure. The amino acid layers in both can be described by the same graph set, although there are differences in detail. Five hydrogen bonds interconnect the lysinium layer and the hydrogen tartrate layer in the L–D complex and in the minor component of the L–L complex. There is uncertainty about one of them in the case of the major component. It is also noteworthy that the *b* dimension, along which the two layers stack, is larger by ~ 0.77 Å in the L–L complex, indicating a somewhat lower packing efficiency. This is presumably related to the disorder in the crystal. Taking all these factors into account, the interaction energy in the L–D complex appears to be slightly better than in the L–L complex. Thus, the two complexes perhaps provide an example of chiral discrimination based on the amplification of a very small energy difference.

The diffraction data were collected using the CCD facility at the Indian Institute of Science under the IRFA programme of the Department of Science and Technology. Financial support from the Indian Space Research Organization through their RESPOND programme is acknowledged. MV is supported by a Distinguished Biotechnologist Award of the Department of Biotechnology, India.

References

Allen, F. H. (2002). *Acta Cryst.* B**58**, 380–388.
Bernstein, J., Davis, R. E., Shimoni, L. & Chang, N.-L. (1995). *Angew. Chem. Int. Ed. Engl.* **34**, 1555–1573.
Bruker (2001). *SMART* and *SAINT*. Bruker AXS Inc., Madison, Wisconsin, USA.
Chandra, N. R., Prabu, M. M., Venkatraman, J., Suresh, S. & Vijayan, M. (1998). *Acta Cryst.* B**54**, 257–263.
Debrus, S., Marchewka, M. K., Baran, J., Drozd, M., Czopnik, R., Pietraszko, A. & Ratajczak, H. (2005). *J. Solid State Chem.* **178**, 2880–2896.
DeLano, W. L. (2002). *The PyMOL Molecular Graphics System.* DeLano Scientific, San Carlos, CA, USA.
Etter, M. C., MacDonald, J. C. & Bernstein, J. (1990). *Acta Cryst.* B**46**, 256–262.
Farrugia, L. J. (1997). *J. Appl. Cryst.* **30**, 565.
Johnson, M. N. & Feeder, N. (2004*a*). *Acta Cryst.* E**60**, o1273–o1274.
Johnson, M. N. & Feeder, N. (2004*b*). *Acta Cryst.* E**60**, o1374–o1375.
Marchewka, M. K., Debrus, S., Pietraszko, A., Barnes, A. J. & Ratajczak, H. (2003). *J. Mol. Struct.* **656**, 265–273.
Prasad, G. S. & Vijayan, M. (1993). *Acta Cryst.* B**49**, 348–356.
Pratap, J. V., Ravishankar, R. & Vijayan, M. (2000). *Acta Cryst.* B**56**, 690–696.
Roy, S., Singh, D. D. & Vijayan, M. (2005). *Acta Cryst.* B**61**, 89–95.
Salunke, D. M. & Vijayan, M. (1981). *Int. J. Pept. Protein Res.* **18**, 348–351.
Saraswathi, N. T., Roy, S. & Vijayan, M. (2003). *Acta Cryst.* B**59**, 641–646.
Saraswathi, N. T. & Vijayan, M. (2001). *Acta Cryst.* B**57**, 842–849.
Saraswathi, N. T. & Vijayan, M. (2002). *Acta Cryst.* B**58**, 1051–1056.
Sharma, A., Thamotharan, S., Roy, S. & Vijayan, M. (2006). *Acta Cryst.* C**62**, o148–o152.
Sheldrick, G. M. (1997). *SHELXS*97 and *SHELXL*97. University of Göttingen, Germany.
Spek, A. L. (2003). *J. Appl. Cryst.* **36**, 7–13.
Suresh, S., Prasad, G. S. & Vijayan, M. (1994). *Int. J. Pept. Protein Res.* **43**, 139–145.
Suresh, C. G. & Vijayan, M. (1983). *Int. J. Peptide Protein Res.* **22**, 129–143.
Suresh, S. & Vijayan, M. (1995*a*). *Acta Cryst.* B**51**, 353–358.
Suresh, S. & Vijayan, M. (1995*b*). *J. Biosci.* **20**, 225–234.
Suresh, S. & Vijayan, M. (1996). *Acta Cryst.* B**52**, 876–881.
Vijayan, M. (1980). *FEBS Lett.* **112**, 135–137.
Vijayan, M. (1988). *Prog. Biophys. Mol. Biol.* **52**, 71–99.